Dynamic Light Scattering and Dynamic Viscoelasticity of Poly(vinyl alcohol) in Aqueous Borax Solutions. 2. Polymer Concentration and Molecular Weight Effects

Norio Nemoto,*,† Akihiro Koike,† and Kunihiro Osaki‡

Department of Applied Physics, Faculty of Engineering, Kyushu University, Hakozaki, Fukuoka 812-81, Japan, and Institute for Chemical Research, Kyoto University, Uji, Kyoto 611, Japan

Received July 27, 1995; Revised Manuscript Received November 28, 1995[⊗]

ABSTRACT: Dynamic light scattering (DLS) and dynamic viscoelastic (DVE) measurements are made on aqueous borax solutions of three poly(vinyl alcohol) (PVA) samples with weight-average degrees of polymerization $DP_W = 600$, 2100, and 2600. The PVA concentration C of the respective samples is chosen to encompass the threshold concentration C^* at which chains start to overlap in pure aqueous solution. The time correlation function of light intensity scattered from the solutions always exhibits the presence of two dominant modes. The decay rate Γ_f of the fast mode is proportional to the square of the scattering vector **q** for all samples, from which the dynamic correlation length ξ_H is estimated. ξ_H is found to change its C and M dependences at the concentration C_N close to C^*. The q dependence of Γ_s of the slow mode varies from $\Gamma_s \sim q^{2-3}$ below C_N to $\Gamma_s \sim q^0$ with a further increase in C. The dynamic scaling law is applied to the former data. The characteristic time τ_s ($\equiv\Gamma_s^{-1}$) obtained for $C > C_N$ increases with M and is in good agreement with the mechanical relaxation time τ_M obtained by fitting DVE data to the Maxwell model with a single relaxation time.

Introduction

In the first paper of this series, hereafter called Part I,[1] we reported that the slowly decaying mode with the decay rate Γ_s, in addition to the fast diffusive mode, appeared in time profiles of the time correlation function $A_q(t)$ of light intensity scattered from aqueous borax solutions of poly(vinyl alcohol) (PVA) with the degree of polymerization DP = 1750, the degree of saponification = 96 mol %, and a weight ratio of PVA to sodium borate = 2/1. At polymer concentration C near but below the threshold concentration C^* at which PVA chains without sodium borate begin to overlap, the slow mode was found to be the diffusive one from $\Gamma_s \sim q^2$ as found for the fast mode. Here q is the magnitude of the scattering vector **q**. At higher C, the slow mode turned out to become the relaxation one characteristic of $\Gamma_s \sim q^0$, being supported by excellent agreement between τ_s ($=\Gamma_s^{-1}$) and the relaxation time τ_M. The latter was obtained fitting dynamic shear modulus data measured to the same samples to the Maxwell model with a single relaxation time.

Dynamical coupling between concentration fluctuation and elastic stress has been found for several systems which form transient viscoelastic networks.[2−9] In the case of the PVA/borax solution, a so-called "didiol" complex is considered to play an essential role for formation of viscoelastic network as a physical cross-linking point between PVA chains at higher C. We may also expect that very large clusters are formed as a result of complex formation at around C^*. If so, the marked change in the q dependence of the slow mode with increasing polymer concentration should be discussed more thoroughly in relation to growth of clusters due to the complex formation and the evolution to a physically cross-linked network with an increase in C above C^*. Since C^* is dependent on PVA molecular weight M or DP, simultaneous measurements of dynamic light scattering (DLS) and dynamic viscoelasticity (DVE) using samples with different molecular weights may provide useful data for elucidation of dynamics of this associating polymer system.

This paper presents DLS and DVE results on three PVA/borax solutions with weight-average degrees of polymerization $DP_W = 600$, 2100, and 2600 in the dilute to the semidilute concentration range. The time correlation function of light intensity scattered from the solutions always exhibited the presence of two dominant decaying modes. The decay rate Γ_f of the fast mode was found to be proportional to the square of the scattering vector **q** for all samples, from which the dynamic correlation length ξ_H was estimated. ξ_H was found to change its C and M dependences at the concentration C_N from $\xi_H \sim C^0M^{0.25\pm0.05}$ to $\xi_H \sim C^{-(0.40\pm0.03)}M^0$. Here C_N is defined as the concentration at the inflection point appearing in the solution viscosity vs C curve. With increasing C, Γ_s also changed its q dependence from $\Gamma_s \sim q^{2-3}$ to $\Gamma_s \sim q^0$ at around C_N. The dynamic scaling law was found to be applicable for q-dependent Γ_s data from their superposition to one master curve in a reduced plot of Γ_s/q^2D_s vs qR_s. Here D_s is the value of Γ_s/q^2 extrapolated to $q = 0$ and R_s the characteristic length of the clusters. In the C region where Γ_s becomes independent of q, the characteristic time τ_s ($\equiv\Gamma_s^{-1}$) increased with M and was in good agreement with the mechanical relaxation time τ_M obtained by fitting DVE data to the Maxwell model with a single relaxation time.

Experimental Section

Materials. The three poly(vinyl alcohol) (PVA) samples used in this study are a gift from Kurary Co., Ltd. The weight-average degrees of polymerization, DP_W, of the samples are 600, 2100, and 2600 with the same degree of saponification of 88.0 mol %, being characterized by the supplier. GPC measurements showed that the molecular weight distribution was the most probable type of distribution. Concentrated stock solutions of PVA and of sodium borate (SB), $Na_2B_4O_7{\cdot}10H_2O$, were separately prepared using dust-free purified water (resistance > 16 MΩ) and made optically clean by filtration

* To whom correspondence should be addressed.
† Kyushu University.
‡ Kyoto University.
⊗ Abstract published in *Advance ACS Abstracts,* January 15, 1996.

0024-9297/96/2229-1445$12.00/0

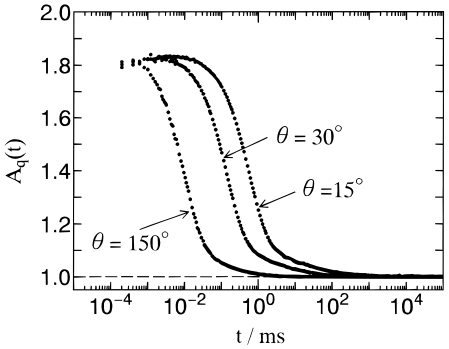

Figure 1. Time profiles of the normalized time correlation function, $A_q(t)$, of light intensity scattered from the PVA/SB system with $DP_W = 2100$ and $C = 1.6$ wt %. Scattering angles θ are 15, 30, and 150° as indicated. The curves exhibit the presence of two dominant decaying modes, both of which shift to the left along the delay time axis with increasing θ.

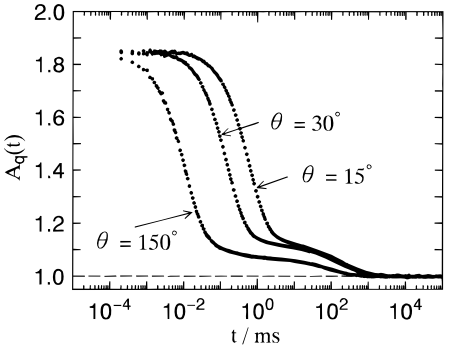

Figure 2. Time profiles of the normalized time correlation function, $A_q(t)$, of light intensity scattered from the PVA/SB system with $DP_W = 2600$ and $C = 2.0$ wt %. Scattering angles θ are 15, 30, and 150° as indicated. The curves exhibit the presence of two dominant decaying modes, in which the fast mode shifts to the left along the delay time axis with increasing θ, while there appears to be no shift in the slow mode.

by a Millipore filter (nominal pore size, 0.22 μm). Prescribed amounts of the two stock solutions were poured into the DLS cell to obtain the solution of desired polymer concentration C by weight. The SB concentration was always adjusted so as to be half that of PVA. Finally, the cell was rotated at 0.2 rpm for about 2 h at 80 °C in order to make samples homogeneous and transparent. More than five solutions with different C were prepared with this procedure for respective PVA samples. The sample code PVA $X-Y$ given in Table 1 represents DP_W as X and C as Y in weight percent for the PVA/SB solutions tested.

Methods. Dynamic light scattering (DLS) measurements were made with a spectrometer (ALV-125) equipped with a multiple τ digital correlator (ALV-5000FAST). A vertically polarized single-frequency 488 nm line of an argon ion laser (Spectra Physics, Beamlock 2060) was used as a light source with an output power of 300 mW. The normalized time correlation function, $A_q(t)$, of the vertical component of the light intensity scattered from the solutions was measured over a range of the scattering angle θ from 15 to 150° at a temperature $T = 25$ °C. It became tremendously difficult to prepare homogeneous solutions with C higher than that listed in Table 1, especially for the highest molecular weight PVA samples. Thus, reliable data were only obtained in a rather restricted C range.

Dynamic viscoelastic (DVE) measurements were made immediately after DLS measurements with a stress-controlled rheometer, CSL100 (Carri-MED, ITS Japan) using a cone-and-plate geometry with a cone diameter of 4 cm and a cone angle of 2°. The semidilute PVA/SB solutions are reported to exhibit the shear-thickening phenomenon as revealed in steady flow and creep measurements.[10−14] The complex modulus was found to be independent of the strain applied when the strain was less than 0.7. In this study, the storage and the loss shear moduli, $G'(\omega)$ and $G''(\omega)$, of the samples were measured at a strain of 0.3 over an angular frequency, ω, from 0.07 to 100 rad/s at $T = 25$ °C. A humidity chamber was used to prevent solvent evaporation.

We performed all measurements within 1 or 2 days after sample preparation. Repeated DLS and DVE measurements after the first run gave the same results, indicating that reduction of the shear viscosity with the elapse of storage time as reported by Maerker and Sinton[15] did not occur in our samples.

Results

DLS Behavior. Data Analysis. The normalized time correlation function, $A_q(t)$, of scattered light intensity exhibited, at first glance, the presence of two dominant decaying modes for all solutions studied as illustrated in Figures 1 and 2. The data in these figures are those obtained for the samples PVA2100-1.6 and PVA2600-2.0, respectively, and indicate that the initial rapid decay of $A_q(t)$ shifts to the left along the delay time axis with increasing scattering angle θ for both samples, while the θ dependence of the slowly decaying component appears quite different between the two samples. We applied the inverse Laplace transformation (ILT), CONTIN, and the multiple exponential function (MEF) methods to obtain a distribution of the decay rate Γ from $A_q(t)$, and also the cumulant method for an estimate of the first cumulant Γ_e, which was used to assess the former three methods.

The ILT and the MEF methods were found to give results consistent with each other and supported by Γ_e data, whereas the CONTIN method could not. We concluded that the decay rate distribution could be best represented by three characteristic decay rates ($\Gamma_f > \Gamma_m > \Gamma_s$) which were obtained from integration of the respective distributions of the decay rate $G(\Gamma_i)$ (i = f, m, s). The amplitude of the medium mode corresponding to Γ_m was always much smaller than those of the other modes; thus values of Γ_m are subject to large experimental uncertainty. Therefore, we shall pay attention to the dependences of the fast and the slow modes on the magnitude $q = (4\pi/\lambda)\sin(\theta/2)$ of the scattering vector **q**, polymer concentration C, and molecular weight in this paper.

The Fast Mode. The q dependence of Γ_f corresponding to the fast mode is shown as a plot of Γ_f/q^2 against q in Figure 3, selecting 8 typical data sets from 22 PVA/SB solutions tested. Γ_f/q^2 is clearly independent of q, which was also found to be applicable for other PVA solution data not shown in the figure. This result indicates that the fast mode is the diffusive mode and the cooperative diffusion coefficient D_c can be estimated as an average of Γ_f/q^2. The dynamical correlation length ξ_H was estimated using the Stokes−Einstein relationship, eq 1.

$$\xi_H = k_B T/6\pi\eta_s D_c \qquad (1)$$

Here the viscosity of pure water was used as η_s, because C of the polymer solutions studied was low in the range of 1.2−4.5 wt % and also ξ_H corresponds to the short-time behavior of concentration fluctuation. Values of D_c and ξ_H are listed in Tables 1−3.

A plot of ξ_H against C shown in Figure 4 reveals that its C and M dependences are different in the two regions which are unambiguously distinguished by a jump of ξ_H at some critical concentration C_N dependent on PVA molecular weight. ξ_H depends on M but is independent of C in the low-C region, whereas it becomes indepen-

Table 1. Experimental Results of the PVA/SB System with $DP_w = 2600$

sample code	C/wt %	pH	$D_c/10^{-7}$ cm^2 s^{-1}	ξ_H/nm	τ_s/s	τ_M/s	G_N/Pa	$D_s/10^{-8}$ cm^2 s^{-1}	R_s/ nm	η_0/Pa s	$A_s/(A_f + A_s)$
PVA2600-1.2	1.2	8.8	5.6 ± 0.2	4.3 ± 0.2				3.5 ± 1.0		0.009 ± 0.001	
PVA2600-1.3	1.3	8.8	5.7 ± 0.2	4.3 ± 0.2				1.5 ± 0.5	33	0.020 ± 0.002	
PVA2600-1.4	1.4	8.8	5.7 ± 0.2	4.3 ± 0.2				0.28 ± 0.10	93	0.060 ± 0.005	
PVA2600-1.5	1.5	8.9	5.0 ± 0.2	4.9 ± 0.3	0.067 ± 0.015	0.070 ± 0.015	10 ± 1			0.50 ± 0.02	0.30 ± 0.02
PVA2600-1.8	1.8	8.8	5.2 ± 0.2	4.7 ± 0.2	0.14 ± 0.015	0.16 ± 0.04	72 ± 5			9.2 ± 0.2	0.34 ± 0.02
PVA2600-2.0	2.0	8.8	5.6 ± 0.2	4.4 ± 0.2	0.29 ± 0.10	0.29 ± 0.10	200 ± 10			35 ± 1	0.37 ± 0.03
PVA2600-2.5	2.5	8.7	6.1 ± 0.2	4.0 ± 0.2	0.53 ± 0.15	0.50 ± 0.20	800 ± 30			260 ± 10	0.50 ± 0.04
PVA2600-3.0	3.0	8.6	6.6 ± 0.2	3.7 ± 0.1	0.91 ± 0.20	1.0 ± 0.20	1500 ± 50			650 ± 50	0.54 ± 0.05

Table 2. Experimental Results of the PVA/SB System with $DP_w = 2100$

sample code	C/wt %	pH	$D_c/101^{-7}$ cm^2 s^{-1}	ξ_H/nm	τ_s/s	τ_M/s	G_N/Pa	$D_s/10^{-8}$ cm^2 s^{-1}	R_s/ nm	η_0/Pa s	$A_s/(A_f + A_s)$
PVA2100-1.2	1.2	8.8	6.0 ± 0.2	4.1 ± 0.2				5.0 ± 1.8		0.0056 ± 0.0002	
PVA2100-1.3	1.3	8.9	6.0 ± 0.2	4.1 ± 0.2				2.9 ± 1.0	40	0.0063 ± 0.0002	
PVA2100-1.4	1.4	8.8	6.1 ± 0.2	4.1 ± 0.2				1.1 ± 0.4	68	0.011 ± 0.001	
PVA2100-1.5	1.5	8.7	5.9 ± 0.2	4.2 ± 0.3		0.018 ± 0.007		0.32 ± 0.10	111	0.017 ± 0.002	
PVA2100-1.6	1.6	8.8	6.1 ± 0.2	4.0 ± 0.2		0.022 ± 0.004		0.27 ± 0.10	118	0.063 ± 0.003	
PVA2100-1.8	1.8	8.9	5.3 ± 0.2	4.6 ± 0.2	0.063 ± 0.010	0.066 ± 0.007	24 ± 2			1.0 ± 0.1	0.28 ± 0.03
PVA2100-2.0	2.0	8.8	5.6 ± 0.2	4.4 ± 0.2	0.13 ± 0.02	0.13 ± 0.02	80 ± 5			6.5 ± 0.5	0.46 ± 0.03
PVA2100-2.5	2.5	8.7	6.0 ± 0.2	4.1 ± 0.2	0.22 ± 0.03	0.20 ± 0.02	390 ± 20			65 ± 2	0.49 ± 0.03
PVA2100-3.0	3.0	8.6	6.4 ± 0.2	3.8 ± 0.1	0.48 ± 0.04	0.48 ± 0.03	1200 ± 100			300 ± 10	0.56 ± 0.05

Table 3. Experimental Results of the PVA/SB System with $DP_w = 600$

sample code	C/wt %	pH	$D_c/10^{-7}$ cm^2 s^{-1}	ξ_H/nm	τ_s/s	τ_M/s	G_N/Pa	$D_s/10^{-8}$ cm^2 s^{-1}	R_s/ nm	η_0/Pa s	$A_s/(A_f + A_s)$
PVA600-1.2	1.2	8.8	8.2 ± 0.2	3.0 ± 0.2				11 ± 2		0.0023 ± 0.0002	
PVA600-2.0	2.0	8.8	8.6 ± 0.2	2.9 ± 0.2				2.3 ± 0.8	40	0.0055 ± 0.0005	
PVA600-2.5	2.5	8.7	7.9 ± 0.2	3.1 ± 0.2				0.50 ± 0.15	70	0.015 ± 0.002	
PVA600-2.7	2.7	8.7	8.1 ± 0.2	3.0 ± 0.2		0.027 ± 0.015		0.36 ± 0.10	90	0.055 ± 0.003	
PVA600-3.0	3.0	8.6	6.6 ± 0.2	3.7 ± 0.2	0.040 ± 0.005	0.038 ± 0.003	40 ± 2			0.9 ± 0.1	0.48 ± 0.05
PVA600-3.5	3.5	8.7	7.2 ± 0.2	3.4 ± 0.1	0.083 ± 0.015	0.076 ± 0.015	390 ± 20			15 ± 1	0.48 ± 0.04
PVA600-4.5	4.5	8.8	7.9 ± 0.2	3.1 ± 0.1	0.21 ± 0.04	0.20 ± 0.04	2900 ± 200			270 ± 10	0.56 ± 0.03

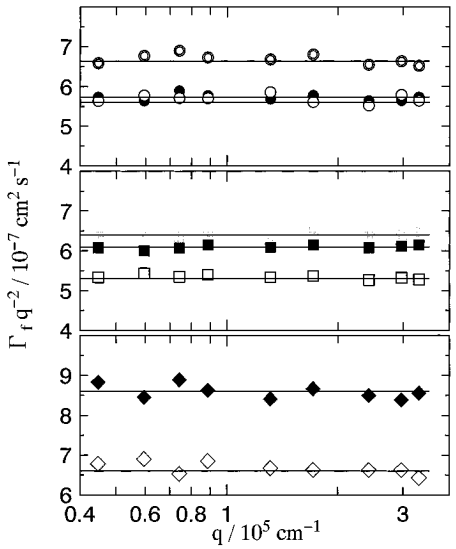

Figure 3. Dependence of the characteristic decay rate, Γ_f, of the fast mode on the magnitude q of the scattering vector shown as a plot of Γ_f/q^2 against q for the eight PVA/SB solutions. From top to bottom: PVA2600-3.0, PVA2600-2.0, PVA2600-1.3, PVA2100-3.0, PVA2100-1.6, PVA2100-1.8, PVA-2600-2.0, and PVA600-3.0.

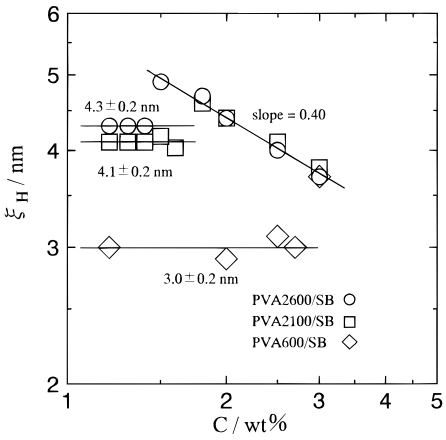

Figure 4. Plot of the dynamical correlation length ξ_H estimated from D_c using the Stokes−Einstein relationship against C. Symbols for DP_W of the PVA samples are (○) 2600, (◇) 2100, and (□) 600. C and M dependences of ξ_H become different at some critical concentration C_N dependent on PVA molecular weight as given by eqs 2 and 3.

dent of M but decreases with increasing C in the higher C region. These dependences are empirically represented as eqs 2 and 3, though the exponent of the M dependence in eq 2 should be reexamined from measurements of other PVA samples with different M.

$$\xi_H \sim C^0 M^{0.25\pm0.05}, \qquad C < C_N \tag{2}$$

$$\xi_H \sim C^{-(0.40\pm0.03)} M^0, \qquad C > C_N \tag{3}$$

Values of C_N have been determined based on the C dependence of the steady flow viscosity as discussed later.

The Slow Mode. The decay rate Γ_s characteristic of the slow mode showed quite different q dependences below and above C_N. Figure 5 gives typical data obtained for solutions with C less than C_N in a logarithmic plot of Γ_s/q^2 against q. The data of other solutions showed a similar trend, though not shown for clarity of the figure. Γ_s/q^2 appears to be almost independent of q at the lowest C of 1.2 wt % studied for three PVA samples with different M. As C increases toward C_N, Γ_s/q^2 still remains constant at low q but starts to increase with q at higher q, and asymptotically becomes

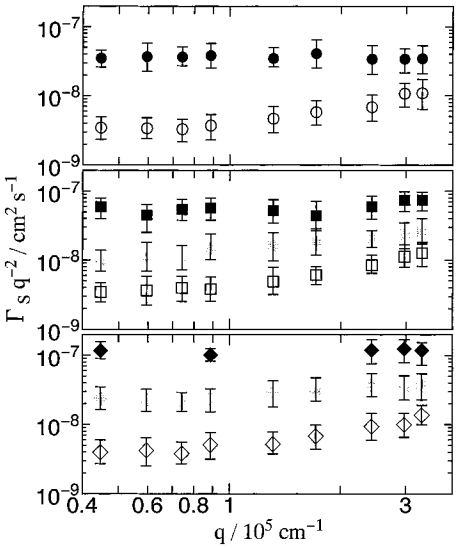

Figure 5. q dependence of the characteristic decay rate, Γ_s, of the slow mode observed for the PVA/SB solutions with $C < C_N$ shown as a plot of Γ_s/q^2 against q. From top to bottom: PVA2600-1.2, PVA2600-1.4, PVA2100-1.2, PVA2100-1.4, PVA2100-1.6, PVA600-1.2, PVA600-2.0, and PVA600-2.7.

proportional to q at C close to C_N. We estimated the characteristic quantity, $D_s = (\Gamma_s/q^2)_{q\to 0}$, from linear extrapolation to $q = 0$, and give D_s values in the three tables.

A similar q dependence of the decay rate was obtained for a single chain of very high molecular weight and was interpreted as intramolecular motions following Rouse-chain dynamics with dominant hydrodynamic interaction.[16−22] Even in the semidilute regime, we obtained a similar result for molecular motions between two adjacent entanglement points of long threadlike micelles which formed a viscoelastic network at very low surfactant concentration.[23] The chain length of the PVA samples used in this study is not long enough for the intermolecular motion to be observed. For the PVA/SB system, instead, we should take into account the possibility of formation of large clusters in this fairly dilute range as a result of intermolecular association due to the didiol complex. Interpretation of the observed q dependence of Γ_s as the relaxation motion inside the cluster may be considered reasonable when the time domain of the slow mode probed by DLS is comparable to the characteristic time τ_{ad} of the association−dissociation kinetics of the complex. This will be discussed later after results of dynamic viscoelastic (DVE) measurements are described.

Γ_s of the solutions with $C > C_N$ is plotted against q in Figure 6. As is clear from the figure, Γ_s is independent of q over the whole measured range of the scattering angle from 15° to 150°, though experimental uncertainty designated by error bars is relatively large. Independence of Γ_s on q was confirmed for seven other solutions, and the characteristic time τ_s as the reverse of averaged Γ_s values are listed in the tables. In Part I of this series of papers, we described that appearance of the relaxation mode in the time correlation function was ascribed to dynamical coupling between concentration fluctuation and elastic stress of the transient network. If this were indeed the case, a uniform viscoelastic network must be formed above C_N, and the characteristic time $\tau_s = \Gamma_s^{-1}$ should be equal to the mechanical relaxation time.

DVE Behavior. Frequency Dependence. We attempted to measure the storage and loss shear moduli,

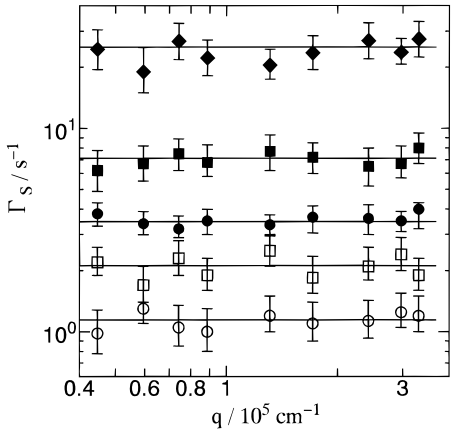

Figure 6. q dependence of the characteristic decay rate, Γ_s, of the slow mode observed for the PVA/SB solutions with $C > C_N$. Symbols are from the top (◆) PVA600-3.0, (■) PVA2100-2.0, (●) PVA2600-2.0, (□) PVA2100-3.0, and (○) PVA2600-3.0.

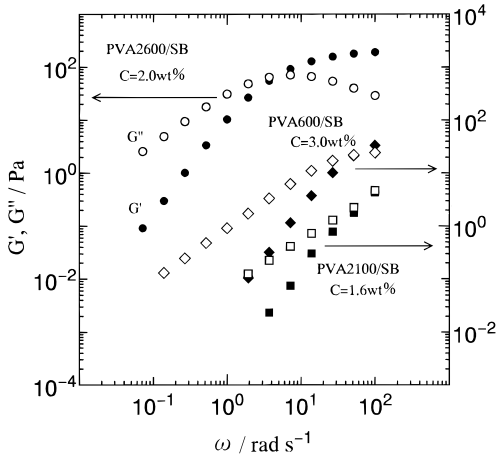

Figure 7. Angular frequency ω dependence of the storage and the loss shear moduli, $G'(\omega)$ and $G^*(\omega)$, of the three solutions whose DP_W and C are given in the figure.

$G'(\omega)$ and $G''(\omega)$, for all solutions but were only successful in measuring the steady-state viscosity η for the solutions far below the respective C_N in the ω range from 0.10 to 10^2 rad/s. Figure 7 shows typical viscoelastic behaviors of the solutions above C_N and of the PVA2100-1.6 solution. G' and G'' are proportional to ω^2 and ω^1 in the low-ω region, respectively, which are characteristic of the steady flow behavior as given by $G'' = \eta\omega$ and $G' = J_e\eta^2\omega^2$. The η and J_e are estimated from the two slopes, and the mechanical relaxation time τ_M is also conveniently evaluated as $\tau_M = J_e\eta$. Alternatively, we may use a Maxwell model with a single relaxation time τ_M and the plateau modulus G_N for data fitting, since the frequency dependences of G' and G'' of the solutions above C_N are characterized by a leveling-off and a maximum of G''.

$$G'(\omega) = \frac{G_N\tau_M{}^2\omega^2}{1 + \tau_M{}^2\omega^2}, \qquad G''(\omega) = \frac{G_N\tau_M\omega}{1 + \tau_M{}^2\omega^2} \tag{4}$$

Values of τ_M, G_N, and η thus obtained are listed in the tables.

The Steady-State Viscosity. The concentration dependence of η is shown for three PVA samples in Figure 8. The sigmoidal shape type of increase in η is characteristic of this associating system. In referring to the DLS results already mentioned, we see that the inflection point in η appears to be located at around C_N

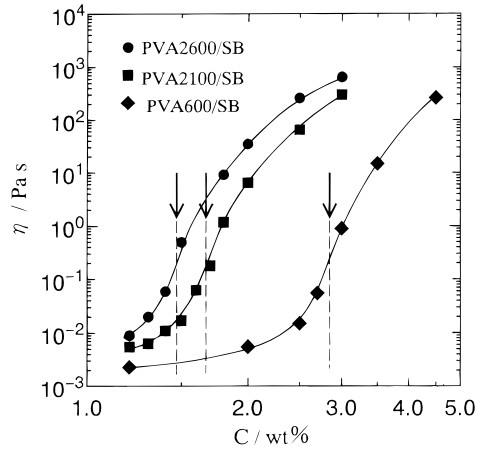

Figure 8. C dependence of the steady-state viscosity η for the three PVA samples. Symbols for DP_W are (●) 2600, (■) 2100, and (◆) 600. An arrow indicates the inflection point in the η vs C curve and is put equal to C_N.

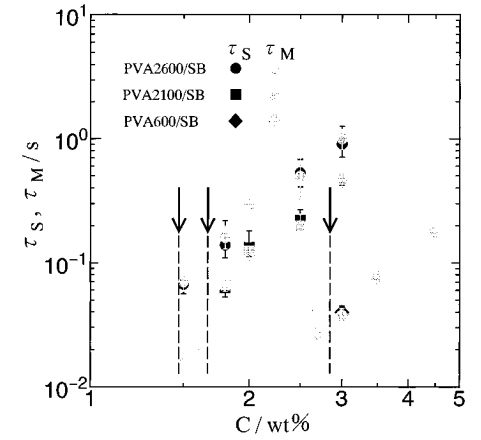

Figure 9. The mechanical relaxation time τ_M and the characteristic time τ_s of the slow mode above C_N indicated as an arrow for each sample are compared. τ_M of three solutions below C_N is also estimated as $\tau_M = J_e\eta$ and shown in the figure. Symbols for DP_W are the same as in Figure 8.

of the respective samples. Since the C_N value could not be definitely located from the DLS results, we put C_N equal to the concentration at the inflection point hereafter. It is to be noted that η seems to take a constant value of 0.2 ± 0.05 Pa s at C_N irrespective of the PVA molecular weight and also that, when the reduced plot of η against C/C_N is made, all data may be superposed on one composite curve. These findings will be throughly discussed after DLS and DVE results are obtained on a couple of PVA samples with different molecular weights. It should be noted that superposition of η data was already discussed for PVA solutions in a mixture of boric acid and sodium hydroxide.[24]

The Mechanical Relaxation Time. We show the concentration dependence of the mechanical relaxation time τ_M in Figure 9, where the data of the solutions below C_N are subject to large experimental uncertainty because of large data scattering of G' values in the flow region. The τ_M of the three solutions above C_N indicated as arrows, respectively, increases concavely to the horizontal axis with C and apparently depends on M at the same C. However, if we attempt to reduce τ_M and C using the corresponding value at C_N and the C_N value, respectively, there seems a possibility that one composite curve may be obtained once again. It seems unnecessary to show the C dependence of G_N because of the relationship of $\eta = G_N\tau_M$ for the single Maxwell type of viscoelasticity. We see from Figures 8 and 9 that η of the three PVA samples increases with C by more than five decades over the C range measured, while τ_M increases with C by less than two decades in the same C range. Therefore the C dependence of G_N is stronger than that of τ_M. The characteristic time τ_s from DLS is also plotted in the same figure for comparison. Excellent agreement between τ_s and τ_M indicates that dynamical coupling between concentration fluctuation and elastic stress of the network is surely present for this associating system.

Discussion

Dynamical Correlation Length. In dilute solutions of neutral polymers, the characteristic length is the radius of gyration R_G (or the hydrodynamic radius R_H), being proportional to $M^{0.5-0.6}$, which only slightly decreases with C. Above the threshold concentration C^*, the static correlation length ξ begins to decrease with C as $\xi \sim C^{-(0.65-1.0)}$. Only one characteristic length is present in good solvent systems, i.e., $\xi \sim \xi_H$. However, we must take into account the presence of the another length which is equal to the average distance between two successive binary contact points in Θ solvent systems, as Adam and Delsanti pointed out.[4] In solutions of associating polymer systems like the PVA/SB solution, didiol complexes are continuously formed and destroyed with the characteristic time τ_{ad} even in the very dilute solution. Therefore, the average distance between the two successive complexes is considered to determine the spatial scale of the pair correlation function between monomeric units and consequently the decay rate of concentration fluctuation in the short-time domain for the PVA/SB system.

Let us consider a PVA chain with the coil size R_G and $DP = N$ in a borax solution with polymer concentration C. The chain is confined in a volume proportional to R_G^3 and associates with other chains with an association number density A_N proportional to CN/R_G^3. We here assume that a stable cluster including this chain is formed when A_N exceeds some critical number with an increase in C, like formation of spherical micelles above the critical micelle concentration, and that the clusters are in thermodynamic equilibrium with free PVA chains. Those clusters are supposed to grow larger and larger absorbing surrounding free PVA chains with further increase in C, while keeping the number of complexes per chain constant. This implies that complex formation is assumed to occur on the cluster surface. Various sizes of clusters will be formed and finally those clusters form a viscoelastic network that is uniform over the whole sample volume at C_N. The average monomer numbers between two successive complexes are proportional to $R_G^3/N \sim M^{0.5-0.8}$ for $R_G \sim M^{0.5-0.6}$; thus $\xi_{ad} \sim M^{0.25-0.4}C^0$ at low C, being consistent with eq 2, if $\xi_{ad} \sim \xi_H$ and the chain takes the unperturbed dimension. Formation of the network which behaves elastically at short time results in a decrease in D_c given as a ratio of the longitudinal bulk modulus to the friction factor per unit volume, which may explain a sudden increase of ξ_H at C_N. ξ_H is no longer dependent on M, but only a function of C for $C > C_N$. Its C dependence should be weaker than that observed for semidilute solutions of neutral polymers, since a number of complexes are already present among overlapped chains.

The above conjecture is not contradictory with values of C^* estimated as the reciprocal of the intrinsic viscosity of PVA in water without sodium borate.[25] We

obtained $C^* = 1.4$, 1.6, and 3.5 wt % for $DP_W = 2600$, 2100, and 600, respectively. As is clear from Figure 4, these values are close to the concentrations where the transition in ξ_H from the eq 2 type of the behavior to the eq 3 type was observed. Eventually, C_N values estimated from the viscosity behavior are found to be very close to C^*.

In order to confirm that the PVA solutions without sodium borate belong to the dilute regime below C^*, we made DLS measurements on pure aqueous solutions of PVA with $DP_W = 600$ in the range of $C = 1.2-3$ wt %. We observed a very slight increase of R_H with C and obtained the value at infinite dilution $R_{H,0} = 7.1$ nm, being reasonable judging from the end-to-end distance of the single PVA chain in the literature.[26] Addition of sodium borate induces association among PVA chains and contraction of the coil size to some extent. Once stable clusters are formed in the dilute regime, the clusters grow in size with increasing C. However, the restriction that A_N is kept constant in the growth process may yield $C_N \sim C^*$ after all. In this connection, it may be noted that C_N roughly decreases with M as $C_N \sim M^{-(0.45\pm0.05)}$, being in harmony with the M dependence of C^* as expected.

As already shown, Γ_s of the slow mode changed its q dependence from q^{2-3} to q^0 at around C_N, and the single Maxwell type of viscoelasticity was observed above C_N. Therefore, we propose that C_N be taken as the characteristic concentration at which the solution structure changes from a collection of large clusters (or microgels) with various sizes, slightly interconnected to each other, to a uniform network extending over the whole sample volume. Recently, we started static and dynamic light scattering measurements as well as viscosity measurements on dilute aqueous solutions of five different molecular weight PVA samples with and without sodium borate, which will provide more information on the effect of complex formation on solution properties and also on the validity of our above-mentioned idea.

The Dynamic Scaling Law. In a previous section, we suggested that the strong q dependence of Γ_s observed for the PVA/borax solutions below C_N was related to the relaxation motions of the PVA chains physically cross-linked by didiol complexes inside the clusters with various sizes and that D_s, a value of Γ_s/q^2 extrapolated to $q = 0$, might represent an average of their translational diffusion coefficients. Thus it seems worthwhile to examine the applicability of the dynamic scaling law to the Γ_s behavior in terms of a reduced plot of Γ_s/q^2D_s vs qR_s, where R_s is the characteristic length of the clusters dependent on C and M. Before making this kind of an attempt, we compared the frequency domain of the slow mode probed by DLS with that of the viscoelastic response spanned by our dynamic viscoelastic instrument. For example, Γ_s of the PVA2100-1.6 solution for which a very strong q dependence was observed ranged from 6 s^{-1} at $\theta = 15°$ to 1600 s^{-1} at $\theta = 150°$. The same solution was found to be an essentially viscous fluid with very small elasticity in the measured ω range of 1−100 rad s^{-1} as characterized by $\tau_M = 0.02$ s or $\omega_0 = 50$ rad s^{-1}. Since the lifetime of the didiol complex, τ_{ad}, should be comparable to τ_M, it is very probable that the observed slow mode originates from concentration fluctuations associated with the consecutive association−dissociation process of the complexes in the clusters.

We need the value of the characteristic length R_s in order to make the reduced plot of Γ_s/q^2D_s vs qR_s. First,

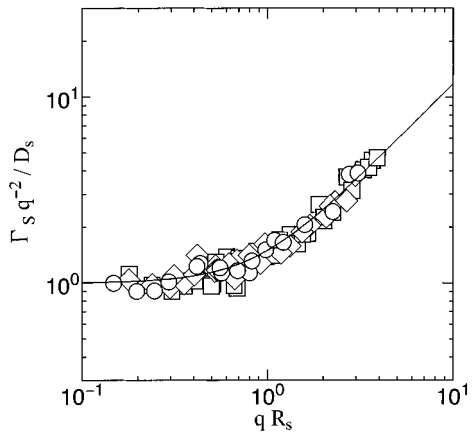

Figure 10. The dynamic scaling law is tested using Γ_s data of the solutions with C below C_N. One composite curve is obtained from superposition of Γ_s/q^2D_s vs q curves on the theoretical curve given by eqs 5 and 6.

R_s was calculated, using the Stokes−Einstein relation, from D_s and the viscosity of pure water, η_w, whose use might be valid far below C_N as an energy dissipation factor representing local friction. With this estimate of R_s, we could superpose all reduced data on one composite curve. However, R_s used for reduction exceeded 1 μm for the samples with C near C_N, casting some doubt on the use of η_w in the case where clusters with various sizes are connected to one another with a few complexes and are coexistent in the solutions. Alternatively, we may treat R_s as an adjustable parameter and superpose Γ_s/q^2D_s vs q curves shifting horizontally on the theoretical curve eq 5, which makes it possible to estimate values of R_s from each shift.

$$\Gamma_s/q^2D_s = F(qR_s) \tag{5}$$

$$F(x) = (3/4x^2)\{1 + x^2 + (x^3 - x^{-1}) \tan^{-1} x\} \tag{6}$$

Equation 6 was originally derived for critical dynamics of low molecular weight liquids by Kawasaki[27] and further applied for chain dynamics of linear flexible polymers in the semidilute regime.[22] It should be kept in mind that there is no justification for eq 5 being applicable to clusters composed of PVA chains associated with physical cross-links, even if reasonable support will be given later for this procedure. Equation 5 may be considered as a simple guide for making superposition.

Figure 10 shows that superposition was successfully achieved for all data except those of the three solutions with $C = 1.2$ wt %, for which it was impossible to find an R_s value because of constant Γ_s/q^2 over the whole q range. R_s values thus obtained are listed in the tables. Hydrodynamic theory predicts that the product of the translational diffusion coefficient D_G and the rotational relaxation time τ_R is only related to the radius of the sphere if the cluster keeps its spherical shape in the flow region and is given by eq 7.[28]

$$D_G\tau_R = 0.667R^2 \tag{7}$$

R was estimated for the three solutions, PVA2100-1.5 and −1.6 and PVA600-2.7, putting $D_G = D_s$ and $\tau_R = \tau_M$ from the tables. Estimated values of R agreed with R_s within experimental accuracy. If the agreement is not fortuitous, the cluster size would become larger than

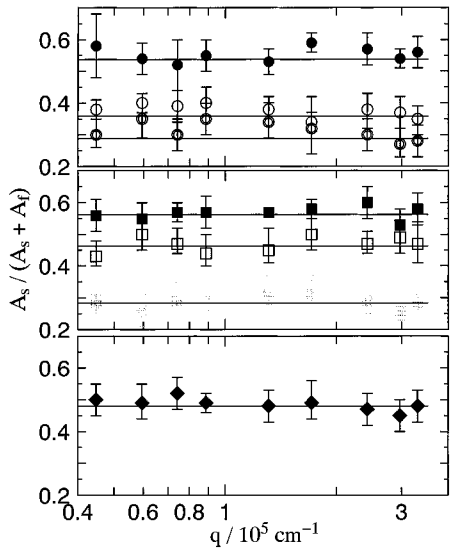

Figure 11. Relative amplitude of the slow mode with q-independent Γ_s, $A_s/(A_s + A_f)$, plotted against q for the seven PVA/SB solutions. From top to bottom: PVA2600-3.0, PVA2600-2.0, PVA2600-1.5, PVA2100-3.0, PVA2100-2.0, PVA2100-1.8, PVA600-4.5, and PVA600-3.0.

100 nm near C_N irrespective of molecular weight of the PVA samples used.

Dynamical Coupling between Concentration Fluctuation and Stress. In Part I, we interpreted such DLS data as shown in Figure 2 in terms of the Doi−Onuki theory,[29] which explicitly took into account dynamical coupling between concentration fluctuation and elastic stress of an entangled network. This phenomenological theory has been developed on the basis of an idea[30] that mass flow or concentration fluctuation in the system creates deformation of the viscoelastic network, which produces a gradient of the elastic stress, and then this gradient affects the diffusive motion of the polymer chain, resulting in slow decay of concentration fluctuation as the network stress relaxes. In a case where the viscoelastic response of the network is described by the Maxwell type of the model with a single relaxation time τ_M and the conditions $\Gamma_f\tau_M \gg 1$ and $\Gamma_f\tau_M \gg \xi_{ve}^2q^2$ are satisfied, where ξ_{ve} is a characteristic length which determines the strength of dynamical coupling, the time profile of the normalized time correlation function of scattered electric field, $E_q(t)$, can be simply expressed as a sum of two exponential functions with three independent variables, Γ_f, τ_M, and A_s (or A_f) as given by eq 8,

$$E_q(t) = A_f \exp(-\Gamma_f t) + A_s \exp(-t/\tau_M) \quad (8)$$

$$A_s = (\xi_{ve}^2q^2/\Gamma_f\tau_M)(1 + \xi_{ve}^2q^2/\Gamma_f\tau_M), \qquad A_f = 1 - A_s \quad (9)$$

When physical cross-links due to complex formation can be regarded as entanglement points which impart topological restriction to global chain motions, eq 8 may be also applicable for the DLS behavior of the PVA/borax system. Indeed, eq 8 correctly explained the previous DLS data in that the fast mode and the slow modes are the diffusion mode ($\Gamma_f = D_cq^2$) and the relaxation mode ($\Gamma_s^{-1} = \tau_s = \tau_M$), respectively. However, the relative amplitude of the slow mode, A_s, decreased with q at low q and asymptotically approached a constant value at high q, whereas the theory predicted a q-independent value.

This work once again confirms the validity of eq 8 to $E_q(t)$ for all the PVA/SB solutions with $C > C_N$. As Figure 11 shows, A_s was found to be independent of q, in agreement with the theoretical prediction. However, A_s calculated from eq 9 increased with C rapidly and the largest value attained was 0.15 for PVA2100-3.0, which is smaller than the corresponding experimental value by a factor of 4. This discrepancy may suggest that an estimate of ξ_{ve} should be done in a different way, which seems to be the only problem left to be solved.

Acknowledgment. The authors are grateful to Kuraray Co. Ltd. for a gift of PVA samples. We also thank Miss M. Nishimura for her help with the viscosity measurements.

References and Notes

(1) Koike, A.; Nemoto, N.; Inoue, T.; Osaki, K. *Macromolecules* **1995**, *28*, 2339.
(2) Amis, E. J.; Han, C. C. *Polym. Commun.* **1982**, *23*, 1043.
(3) Nemoto, N.; Makita, Y.; Tsunashima, Y.; Kurata, M. *Macromolecules* **1984**, *17*, 2629.
(4) Adam, M.; Delasanti, M. *Macromolecules* **1985**, *18*, 1760.
(5) Brown, W.; Nicolai, T.; Hvidt, S.; Stepanek, P. *Macromolecules* **1990**, *23*, 357.
(6) Nicolai, T.; Brown, W.; Hvidt, S.; Heller, K. *Macromolecules* **1990**, *23*, 5088.
(7) Nystrom, B.; Walderhaug, H.; Hansen, F. K. *J. Phys. Chem.* **1993**, *97*, 7743.
(8) Berry, G. C. *Adv. Polym. Sci.* **1994**, *114*, 233.
(9) Nemoto, N.; Kuwahara, M.; Yao, M.-L.; Osaki, K. *Langmuir* **1995**, *11*, 36.
(10) Perzon, E.; Richard, L.; Lafuma, F.; Audebert, R. *Macromolecules* **1988**, *21*, 1126.
(11) Sato, T.; Tsujii, Y.; Fukuda, T.; Miyamoto, T. *Macromolecules* **1992**, *25*, 5970.
(12) Nickerson, R. F. *J. Polym. Sci.* **1971**, *15*, 111.
(13) Shibayama, M.; Sato, M.; Kurokawa, H.; Nomura, S.; Wu, W. L. *Polymer* **1988**, *29*, 336.
(14) Inoue, T.; Osaki, K. *Rheol. Acta* **1993**, *32*, 550.
(15) Maerker, J. M.; Sinton, S. W. *J. Rheol.* **1986**, *30*, 77.
(16) Akcasu, A. Z.; Benmouna, C. C.; Han, C. C. *Polymer* **1980**, *17*, 541.
(17) Tsunashima, Y.; Nemoto, N.; Kurata, M. *Macromolecules* **1983**, *16*, 1184.
(18) Nemoto, N.; Makita, Y.; Tsunashima, Y.; Kurata, M. *Macromolecules* **1984**, *17*, 425.
(19) Tsunashima, Y.; Hirata, M.; Nemoto, N.; Kurata, M. *Macromolecules* **1987**, *20*, 1992; **1988**, *21*, 1107.
(20) Ferry, J. D. *Viscoelastic Properties of Polymers*; John Wiley: New York, 1980.
(21) de Gennes, P.-G. *Scaling Concepts in Polymer Physics*; Cornell University Press: Ithaca, NY, 1979.
(22) Doi, M.; Edwards, S. F. *The Theory of Polymer Dynamics*; Oxford University Press: Oxford, 1986.
(23) Nemoto, N.; Kuwahara, M. *Langmuir* **1993**, *9*, 419.
(24) Kurokawa, H.; Shibayama, M.; Ishimaru, T.; Nomura, S.; Wu, W.-L. *Polymer* **1992**, *33*, 2182.
(25) Matsumoto, M.; Ohyanagi, Y. *Koubunnsi Kagaku* **1960**, *17*, 191 (in Japanese).
(26) Brandrup, J.; Immergut, E. H. *Polymer Handbook*, 3rd ed.; Wiley-InterScience: New York, 1989.
(27) Kawasaki, K. In *Critical Phenomena*; Green, M. S., Ed.; Academic Press: New York, 1971; p 342.
(28) Tanford, C. *Physical Chemistry of Macromolecules*; John Wiley: New York, 1961; Chapter 6.
(29) Doi, M.; Onuki, A. *J. Phys. II Fr.* **1992**, *2*, 1631.
(30) Brochard, F. *J. Phys. Fr.* **1983**, *44*, 39.

MA951101Y